A process-based model simulating the life cycle of *Culex pipines* s.s./*Cx. torrentium* in Germany

Rauhöft L., Duve P., Martins Afonso S.M., Jöst H., Șulețco T., Sauer F.G., Lühken R.

Bernhard Nocht Institute for Tropical Medicine, Hamburg, Germany

Abstract

Mosquitoes are well known for their ability to transmit pathogens, including various arthropod-borne viruses (arboviruses) that are of veterinary and medical interest. The threat of (re-)emerging arboviruses in Europe is increasing due to globalization and climate warming. This also applies to temperate regions, where the transmission of viruses is becoming possible due to an increase of the ambient temperature, i.e. shortening of the extrinsic incubation period. *Culex pipiens* s.s./*Culex torrentium* are the primary vectors of Usutu virus and West Nile virus in Europe and is commonly found in and around human settlements. The prediction of spatial-temporal abundance allows for the early assessment of arbovirus transmission risk and the organization of intervention methods, such as vector control. A process-based model was developed to predict the spatial-temporal occurrence of *Cx. pipiens* s.s./*Culex torrentium* in Germany. The model output is driven by local rainfall and temperature data provided by the European re-analysis and observations for monitoring (E-OBS) data set. Evaluated with field data from over 123 sampling sites, the model is capable of pinpointing the peak in abundance. The mean offset of the simulated and observed peak is -3.16 (CI95=-9.73-3.4) and does not significantly differ from zero ($t_{(145)}$=-0.95, p-value=0.34). One third of the sampling sites showed a significant positive Pearson correlation between simulated and observed mosquito abundance and there is an overall significant linear relationship (LM: adj. R^2=0.24, $F_{(1,\ 3434)}$. The model is also capable of predicting population dynamics for entire Europe, as tested for Moldavia, Ireland, Sweden and Spain. This process-based model can be used to simulate vector control measurements or the impact of increasing temperatures in cause of climate warming.

Introduction

Mosquitoes are important vectors of pathogens. Malaria parasites and dengue virus have the highest relevance on the global scale estimated to result in more than 500 million annual cases predominantly in tropical and subtropical regions (Brady et al., 2012; WHO et al., 2022). However, especially due to climate warming, mosquito-borne pathogens also emerge in Central Europe, e.g. West Nile virus (WNV) and the Usutu virus (USUV) (Cadar et al., 2017; Ziegler et al., 2019). Since the first emergence of USUV (2011/2012) and

WNV (2018) in Germany, both viruses are regularly detected in mosquitoes, horses, birds and humans (Becker et al., 2012; Ziegler et al., 2020). The main vectors for USUV and WNV are *Culex pipiens* s.s./*Cx. torrentium* (Jansen et al., 2019). These species are highly widespread in Europe and have broad host feeding patterns, including birds, non-human mammals and humans, making them good bridge vectors (Wehmeyer et al., 2024).

Mosquito collections provide the foundation to identify the spatial-temporal risk of mosquito-borne pathogen transmission. Thereby, mosquitoes are usually collected with CO_2-traps in the field and subsequently identified and screened in the laboratory. Due to substantial manual labour and high financial costs, surveying at the necessary temporal and geographical resolution needed to monitor newly emerging pathogens is neither feasible nor sustainable. Process-based models are a useful tool, using mathematical equations to simulate scientific phenomena, i.e. here the life cycle of *Culex pipiens* s.s./*Cx. torrentium*. Driven by environmental factors such as temperature and rainfall these models enable the estimation of spatial-temporal differences in mosquito abundances. Several process-based models for mosquitoes have been published for Europe with a focus on the Mediterranean region, i.e. Italy or Southern France. In the publication of Ezanno et al. (Ezanno et al., 2015), model parameters for three different species were validated. Namely, *Anopheles hyrcanus*, *Cx. pipiens* s.s./*Cx. torrentium* and *Aedes caspius*. The models were validated with field data from two sampling sites in France collected over two consecutive years with Pearson correlations between 0.75 to 0.89. Additionally in southern France, an *Aedes albopictus* model was published correlating the number of newly laid eggs averaged over 15-50 ovitraps at 6 sampling sites (Tran et al., 2013). Correlations were calculated ranging from 0.73 to 0.93. In another study from northern Italy, aggregated trap data from 24 traps dispersed over 987 km^2 and ran over 12 consecutive years were averaged by week and correlated to a *Cx. pipiens* s.s./*Cx. torrentium* model. While no formal significance test was made, 90% of the weekly averages laid within the 2.5-97.5% quantile of the model prediction (Marini et al., 2016). Thus, a large scale, site-specific evaluation of process-based models for *Cx. pipiens* s.s./*Cx. torrentium* is missing.

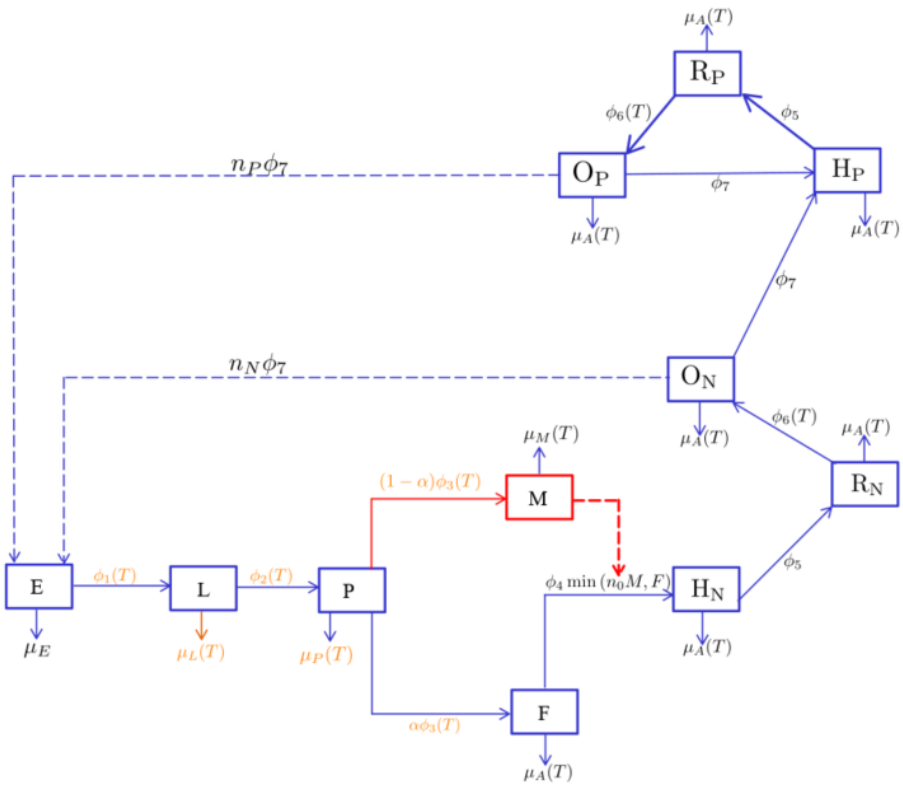

Figure 1: Flow chart diagram for the process-based model for the mosquito life cycle of *Cx. pipiens* s.s./ *Cx. torrentium*. Boxes represent compartments or different stages, while solid lines represent the development from one stage to another. Dashed lines represent the transition from one state to another. Red highlights a new compartement, wich were added to the initial model. Orange indicates the adjusted transition and mortality rates.

In this work, we consider a process-based model for the life cycle of *Cx. pipiens* s.s./*Cx. torrentium* in Germany. We adapted the generic model for *Ades albopictus* first proposed by Cailly et al. (2012) and further extended to other species by Ezanno et al. (2015), allowing to model the densities of mosquitoes at different life stages. We made different adjustments to the model structure. Firstly, we extended the model by a compartment that predicts the number of emerging males to include the mating behaviour of females and males. The inclusion is relevant, as reared males are used in different control measures such as the use of sterile insect techniques (SIT) or *Wolbachia* infected males, among others (Anguelov et al., 2017; Bourtzis et al., 2014) . Secondly, additional adaptions were conducted for the temperature-dependent

transition function from egg to larvae ($\phi_1(T)$), larvae to pupae ($\phi_2(T)$) and pupae to emerging ($\phi_3(T)$) and mortality functions for larvae ($\mu_L(T)$) and pupae ($\mu_P(T)$), increasing the temperature range in which the model is applicable and thus, the geographic range of usability. Thirdly, our model does no longer rely on a predefined favourable and unfavourable seasons, triggering the start and the end of the overwintering period. This predefined binary variable, based on expert knowledge, triggers one of two sets of equations where mosquitoes are either active or in diapause. The new process-based model was validated with field-data for the whole country and agro-climatic regions of Germany, including the start, end and peak of annual mosquito activity. Furthermore, the model was compared against a correlation against a model including only temperature and the variable importance for the overall mosquito dynamic and the population peak was analysed using a sensitivity analysis.

Methods

Mathematical model for the life cycle of *Cx. pipiens* s.s./*Cx. torrentium*:

The model consists of the different mosquito densities of aquatic stages: egg (E), larval (L), pupal (P), and adult stages: male (M), female (F), nulliparous host-seeking female (H_N), nulliparous resting female (R_N), nulliparous oviposition site-seeking female (O_N), parous host-seeking female (H_P), parous resting female (R_P) and parous oviposition site-seeking females (O_P).

Transition from one to the next aquatic stage is temperature-dependent ($\phi_1(T)$, $\phi_2(T)$, $\phi_3(T)$), same as the mortality rates for larvae and pupae ($\mu_L(T)$, $\mu_P(T)$). Rainfall increases the number of available breeding sites. The competition of resources within the breeding site will lead to a density-dependent larva mortality of $\mu_L(T)\left[1+\frac{\mu_L(T)}{K_L}\right]$ Ezanno et al. (2015); Legros et al. (2009); Lutambi et al. (2013). A proportion α of pupa mosquito develops into emerging females or males $(1-\alpha)$. Females mate with male mosquitoes before progressing to the host-seeking stage. One assumption of this model is that all female mosquitoes mate before they seek for a blood meal, and that the females are autogenous, and they have the ability to produce an offspring. As in Ezanno et al. (2015), it is assumed that females only mate once. Males can mate several

times in their life span, i.e. Asman (1975) showed that under laboratory conditions male *Cx. pipiens* s.s./*Cx. torrentium* mosquitoes can inseminate up to 8 females over 21 days. Thus, the number of females who get fertilized by males is highly dependent on the population density of sexually active male mosquitoes. As modelled by Anguelov et al. (2017), when there is an abundant number of males in the environment, all females will get inseminated and will progress to the host-seeking stage. On the other hand, when sexually active males in the environment are scarce, the number of females that get inseminated and progress to the host-seeking stage is proportional to the number of available males multiplied by the number of females each male can inseminate denoted as $n_0 M$, where n_0 is the number of females each male inseminates. After mating, female mosquitoes progress to the host-seeking stage at a temperature-dependent rate ϕ_4. After a successful bite, female mosquitoes rest at a rate of ϕ_5 before they start seeking an oviposition site to lay eggs at a rate of $\phi_6(T)$. After depositing eggs at a rate of ϕ_7, female mosquitoes become parous adults. The cycle repeats until the mosquito dies and is removed from the population.

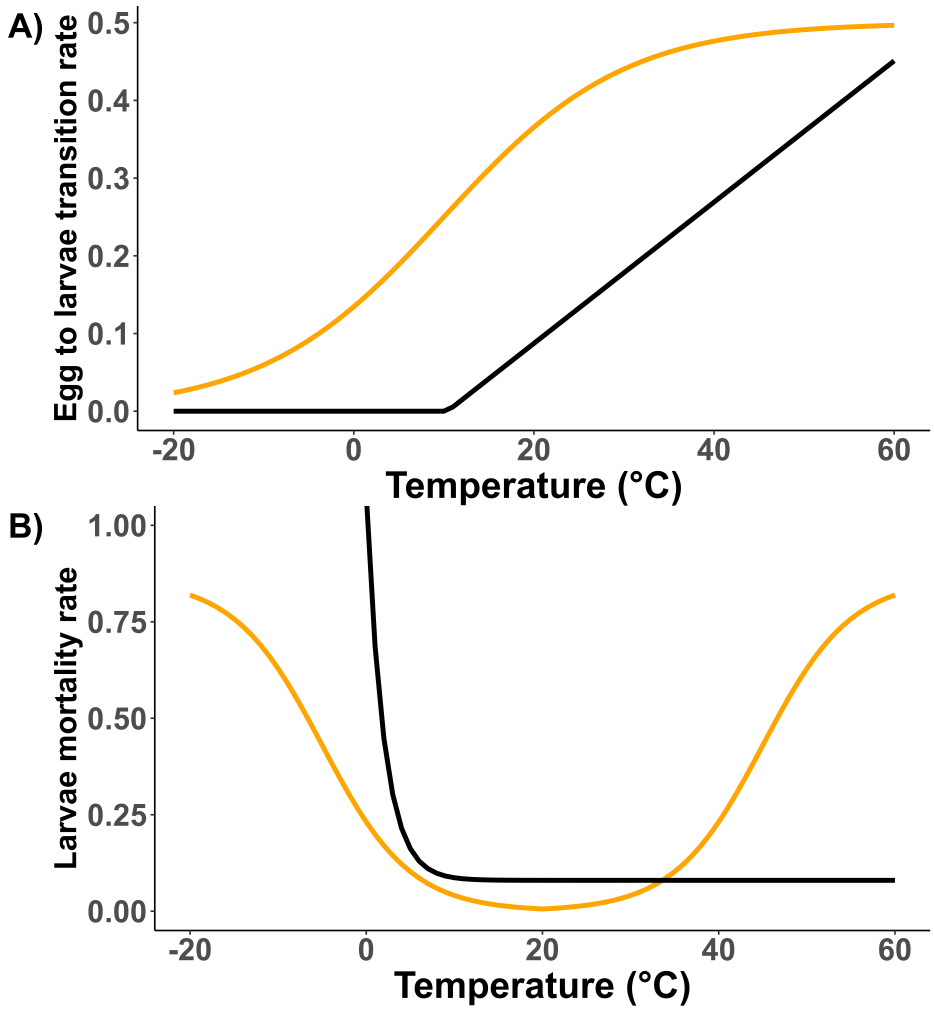

Figure 2: Comparison of the original (Black) and new (Orange) temperature dependent transition rates (A) and mortality rates (B).

Validation:

Data for the validation of the mechanistic model was acquired from two different projects where voluntary helpers ran CO2-mosquito traps on weekly, bi-weekly or daily basis from April until October in the years 2016-2017 and 2021-2023. All female mosquitoes were identified by morphology as *Cx. pipiens* s.s./*Cx. torrentium* using the taxonomic key by Becker et al. (2020). Additionally, the blood-fed status of the caught mosquitoes was assessed using the Sella score (Detinova et al., 1962), categorizing mosquitoes as unfed (Sella score 1) or as blood-fed from freshly engorged to gravid (Sella score 2-7). Only sampling sites with more than six data points and a total capture of more than 30 mosquitoe specimen were analysed, since we

consider this the minimum threshold to accurately depict a seasonal dynamic. Only female mosquitoes were chosen with a Sella score of 1, since these are the specimens that are considered being host-seeking. After sub-setting, the validation dataset consisted of 123 sampling sites (Table 3) with 78271 caught *Cx. pipiens* s.s./*Cx. torrentium* females (mean per day= 22.78, 95% confidence interval (CI95%)=18.45-27.11). Mean daily temperature and mean daily rainfall data (European re-analysis and observations for monitoring, E-OBS, v29.0e) were obtained from http://www.ecad.eu (Cornes et al., 2018) and extracted for each sampling site for 2015-2023. For each sampling site and date, the sum of nulliparous and parous host-searching mosquitoes were compared with data from the field. Relative abundances were calculated, dividing each data point by the yearly maximum for the field data and model output, respectively. Pearson correlations coefficients between the absolute and relative abundances were calculated for each sampling site. The offset in days between the peaks was calculated as field date minus model date. A student's t-test was used to test if the mean offset differs significantly from zero. Additionally, the mean and median offset of the peak were calculated. The same was done for the begin and end of the season, defined as the time point where the number of mosquitoes firstly and lastly exceeded 1% of the corresponding seasonal peak. Validation against all available data were conducted with a linear model of the number of host-searching female mosquitoes from the model and the log1p transformed number of field-collected female mosquitoes with a Sella score of one. Because the model is strongly influenced by temperature, we also used a linear model to examine whether it provided any advantage over simply predicting mosquito abundance based solely on temperature data. A Student's t-test was used to determine if the correlation between the model's predictions and actual mosquito counts from field data was significantly stronger than the correlation between temperature alone and field data. Additionally, we aggregated the data within five distinct agro-climatic zones and correlated the averaged field data and model output (Ceglar et al., 2019). The advantage of these zones is that they incorporate growing season length and active temperature sum . These values are not so prone to be influenced by short extreme weather conditions, like heatwaves, but rather give a long-term effect of cumulative climatic conditions. Lastly, all transition rates within the process-based model were extracted and used to calculate the developmental time to reach the next life stage. A seven-day average temperature at the beginning of each life stage was used for calculation. In this manner we calculated a maximum possible

number of consecutive generations per season and ran this over the entire E-OBS raster for the years 2016 to 2023. These were then visualised in form of a raster map.

Sensitivity analysis:

To gain insights into factors that influence the peak of the population of host seeking adults (sum of nulliparous and parous females) and the general phenology of the population of host-seeking adults throughout the simulation period, we conducted a sensitivity/uncertainty analysis. Thereby, the parameters are resampled using the Latin Hypercube Sampling (LHS) method, which is an efficient stratified Monte Carlo sampling that allows for simultaneous sampling of the multi-dimensional parameter space (Blower and Dowlatabadi, 1994; Hoare et al., 2008). The simulation is carried out for a period of 3 years, with 1000 simulations per run. Partial rank correlation coefficients (PRCCs) are computed for each selected input parameter and the output variables (peak of host seeking females and entire host seeking population) for the entire simulation period.

Software:

All computational analysis was performed in R (Version: 4.2.2) using the R-Studio IDE (Version:2022.12.0) (R Core Team, 2016). Additionally, functions from the following packages were used for data preparation, visualization and analysis: dplyr (Wickham et al., 2023a), tidyr (Wickham et al., 2024), ggplot2 (Wickham, 2016), scales (Wickham et al., 2023b), lubridate (Grolemund and Wickham, 2011), rstatix (Kassambara, 2023), stringr (Wickham, 2023) and knitr (Xie, 2013).

Results

The process-based model resulted in a seasonal dynamic for each sampling site over the entire time period. The output showed a seasonal dynamic for each life stage (Figure 3 B & C). The overwintering life stages depicted by the model are gravid females and males (Figure 3 C. The timing in host-seeking females varied by sampling site, ranging from late July to mid-September. There was a significant positive Pearson correlation between the model output and field data found at 45 sampling sites, while the remaining 78 sites were not significantly correlated. The linear model showed a significant relationship between the host-seeking

mosquitoes predicted by the model and the captured mosquitoes (LM: adj. R^2=0.24, $F_{(1,\ 3434)}$= 1095.22, p-value= <0.0001). Thereby, the linear model explains more variation in the field captures than a linear model relating the field captures to the temperature data alone The linear model relating the field data merely to the corresponding data also shows a significant relationship (LM: adj. R^2=0.14, $F_{(1,\ 3434)}$= 543.73, p-value= <0.0001). Comparing the Pearson correlations of field data to either the process-based model and the temperature alone, for each sampling site, reveals a significantly higher correlation an the side of the model (($t_{(242.16)}$=4.6, p-value=<0.0001)

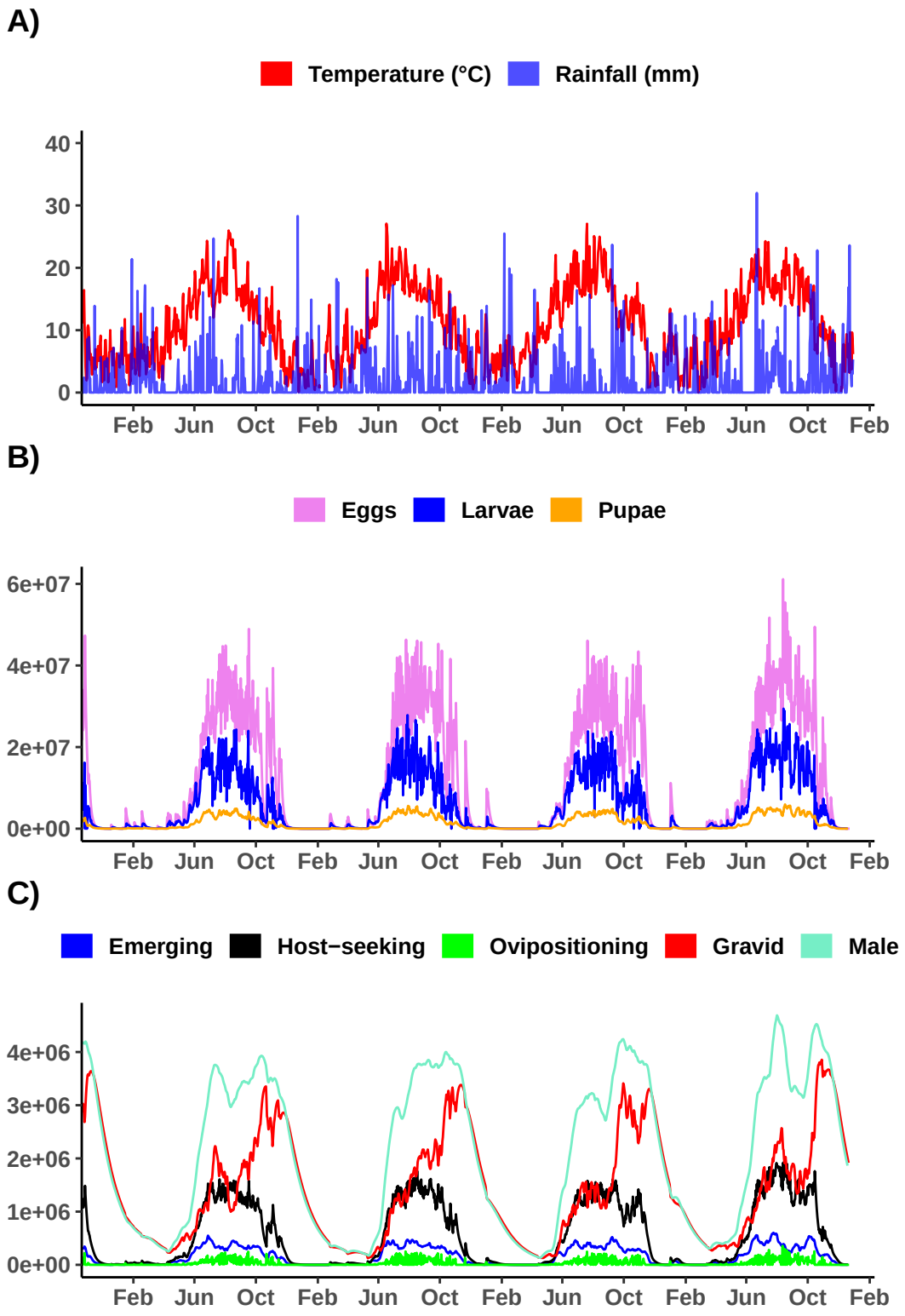

Figure 3: Model output for a single sampling site in Hamburg, Germany divided into B) aquatic life stages, C) adult life stages (nulliparous and parous mosquitoes were summarized) and C) corresponding environmental data between year 2020 and 2023

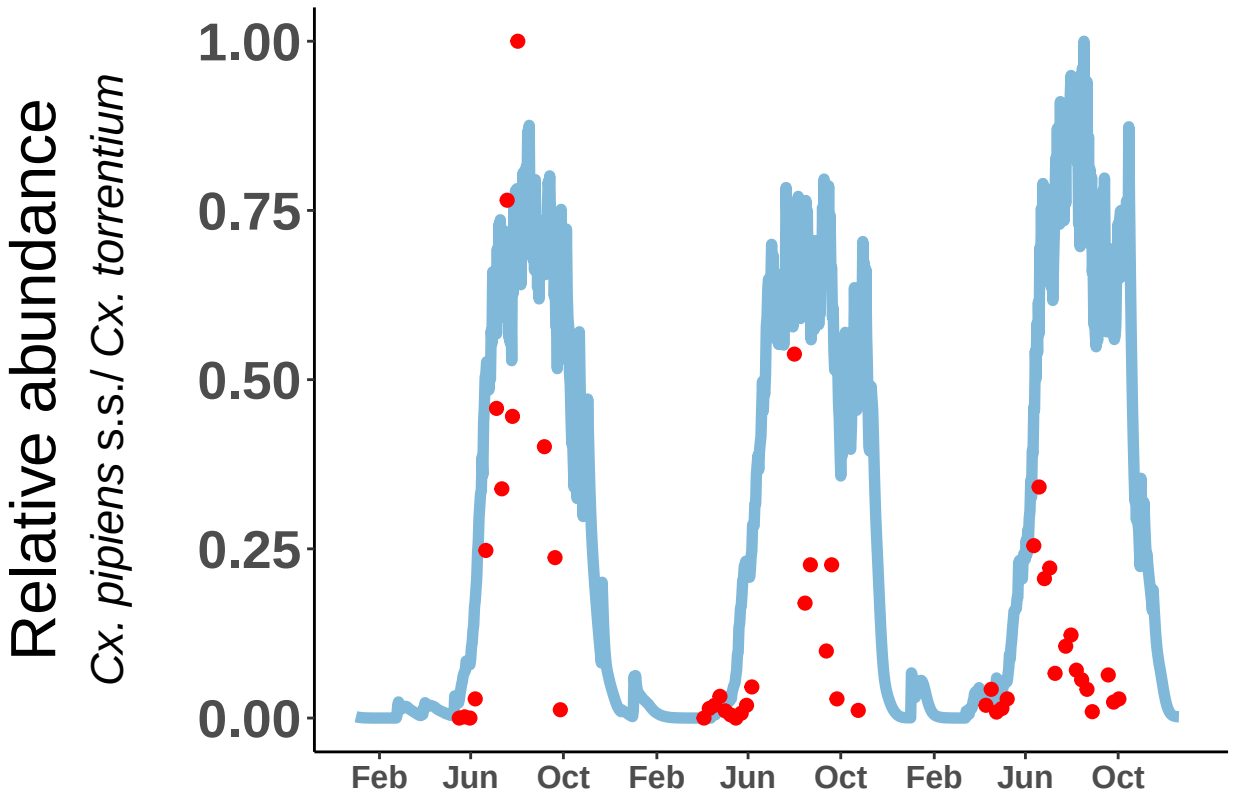

Figure 4: Daily relative model output of the relative abundance of *Cx. pipiens* s.s./ *Cx. torrentium* (blue) and weekly averaged field data (red), shown for a single sampling site in Hamburg, Germany between year 2021 and 2023

The mean offset of abundance peak between the model and field data was -3.16 (CI95=-9.73-3.4) days (Figure 5 A), i.e. on average the peak day predicted by the model lags behind the peak observed in the field data by 3.16 days. The median offset was 0 days. The Student's test shows that the offset does not significantly deviate from zero ($t_{(145)}$=-0.95, p-value=0.34). The mean offset for the start of the season was 26.66 (CI95=22.41-30.91) (Figure 5 b). The median offset of the start of the season is 21.5 days. Therefore, the model is significantly before the observations in the field ($t_{(145)}$=12.4, p-value=<0.0001). The mean offset for the end of the season is -13.5 (CI95=-16.68–10.32 (Figure 5 C). The median offset of the start of the season is 0 days. Hereby, the model is significantly lagging behind the field data($t_{(145)}$=-8.39, p-value<0.0001).

Separating Germany in agro-climatic regions resulted in the majority of sampling sites in the Maritime North, followed by Pannonial and Continental regions (Figure 6). The aggregation of field data and model

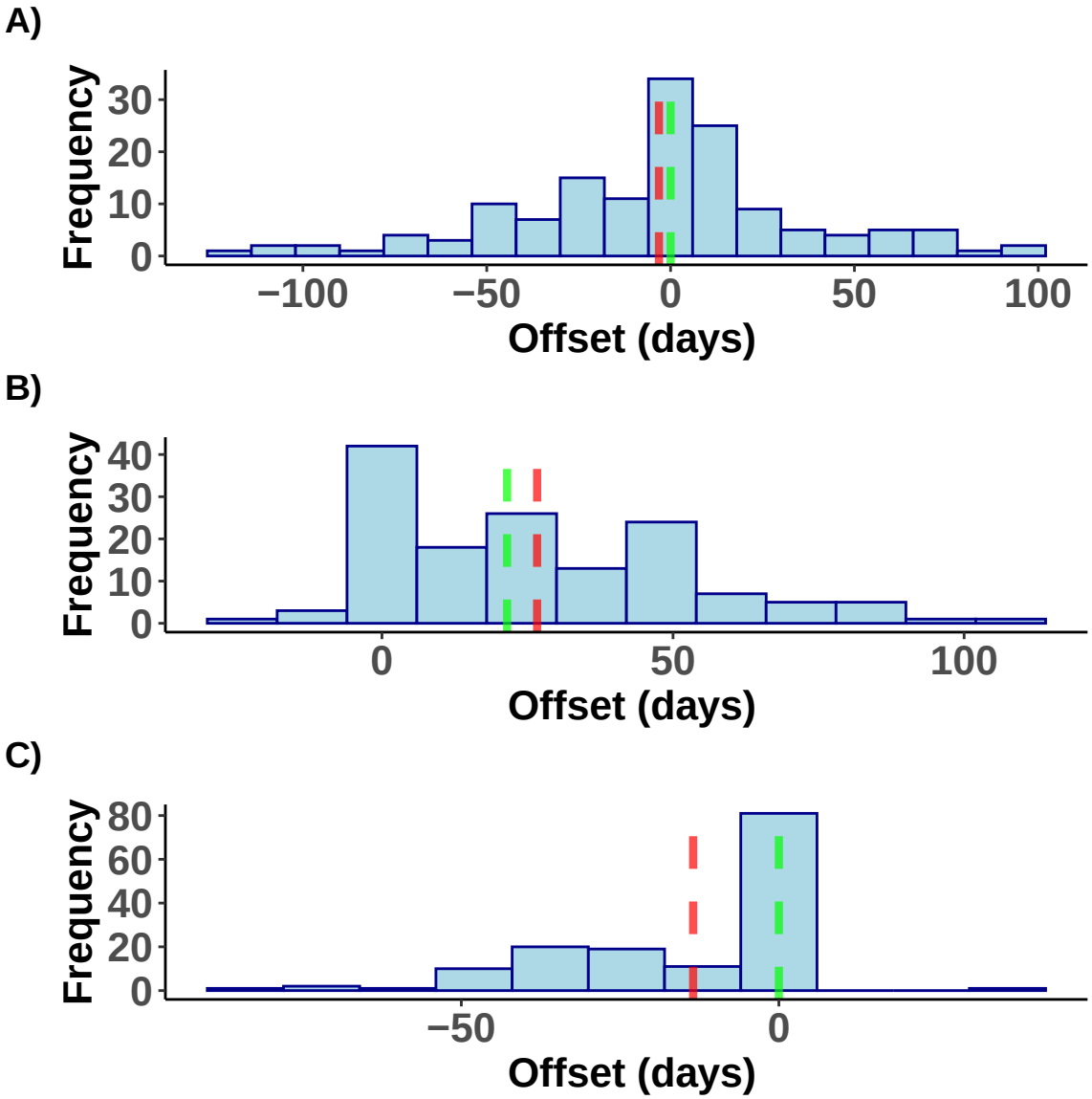

Figure 5: Histogram showing the distribution of the offset between the end of the season according to field data compared to the model. The red-dashed line is the mean- and the green-dashed line is the median offset.

output for these regions resulted in 14 correlations of which 11 had a significant correlation with coefficients ranging from 0.4 to 1 (mean =0.59) (Table 2).

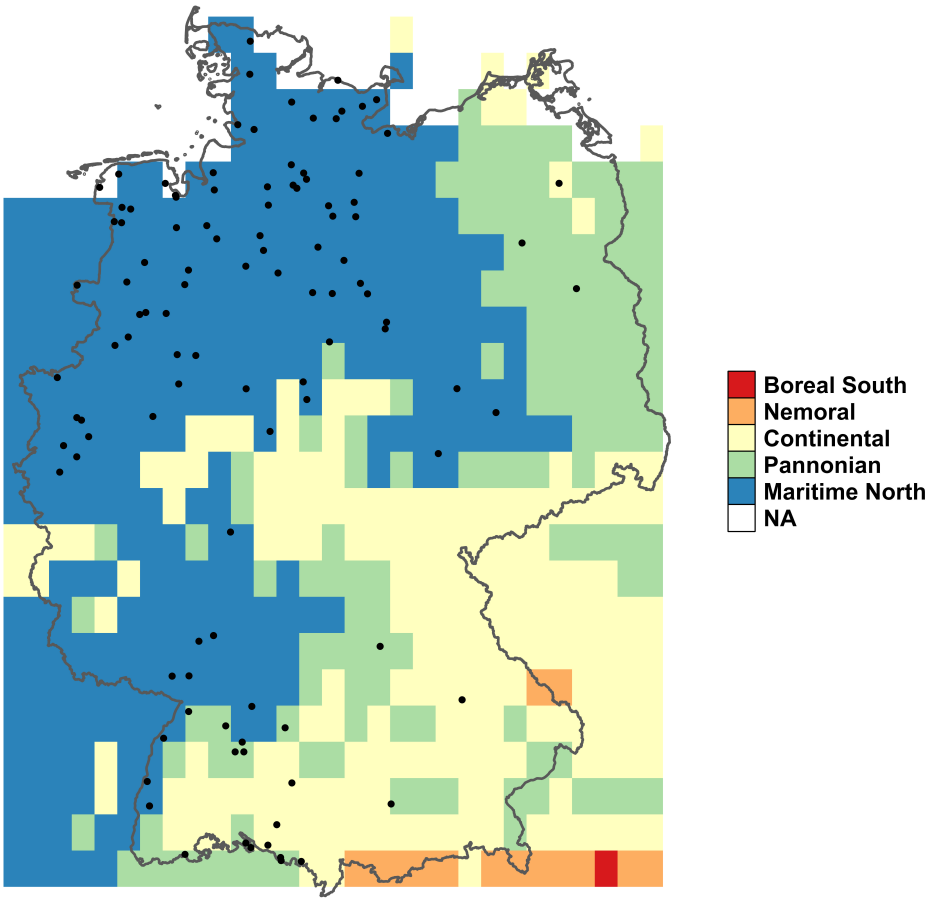

Figure 6: Raster map depicting the agro-climate zones present in Germany. Dots indicate sampling sites.

The model was able to capture the phenology for sites outside of Germany (Figure 7). While for Oulu (Sweden) the mosquito season is short, resulting in a single sharp peak of abundance per year, the duration of high mosquito abundance was longer for Chisinau (Moldavia), Malaga (Spain) and Dublin (Ireland). The longest time period of high mosquito abundance can be seen for Malaga (Spain) where the population decreases sharply during the winter, before it quickly recovers.

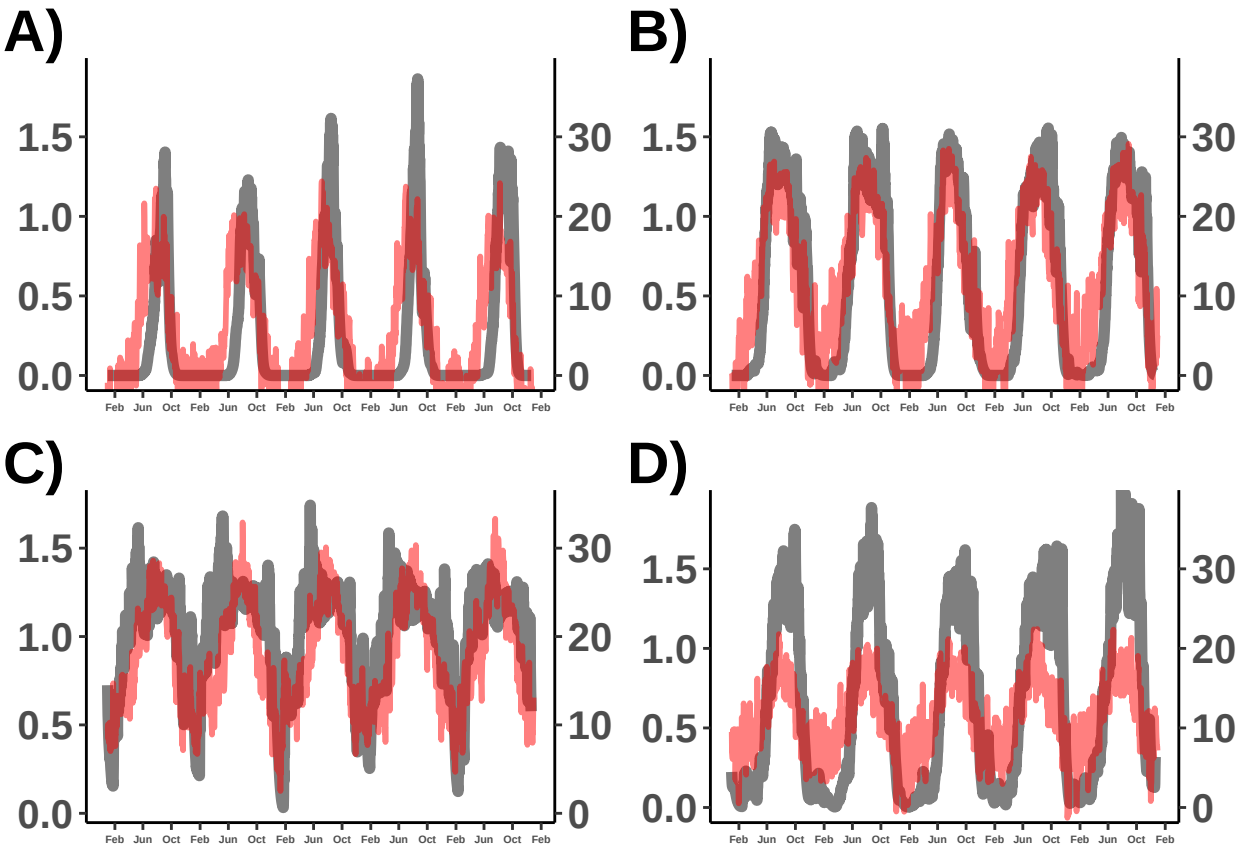

Figure 7: Phenology of host-searching *Cx. pipiens* s.s./ *Cx. torrentium* in millions (grey) depicted by the process-based model from 2019-2023, including the ambient daily average temperature (red) for A) Oulu, Sweden B) Chisinau, Moldavia C) Malaga, Spain and D) Dublin, Ireland (left scale: abundance in million; right scale: temperature in °C)

Table 1: Summary statistics for the correlation analysis for absolute abundances, relative abundances and the temperature for all sampling sites sampled in a high temporal resolution

ID	P-value model	Estimate model	P-value temperature	Estimate temperature	Capture days	Captured mosquitoes	NA	NA
1.PG	0.0000	0.4511	0.0000	0.4574	0.0000	0.4616	112	1927.1817
10.PG	0.0000	0.3947	0.0000	0.3947	0.0029	0.2483	142	627.3571

ID	P-value model	Estimate model	P-value temperature	Estimate temperature	Capture days	Captured mosquitoes	NA	NA
3.PR	0.0000	0.4965	0.0446	0.2581	0.0000	0.5066	61	153.4952
8.PG	0.0000	0.2949	0.0000	0.3005	0.0000	0.3186	544	4158.0000
3.PG	0.0001	0.3811	0.0000	0.4662	0.0001	0.3765	104	1179.9500
1.PR	0.0028	0.2976	0.0028	0.2976	0.1393	0.1497	99	569.8929
8.PR	0.0038	0.2913	0.2758	0.1118	0.0006	0.3415	97	855.7619
30.PG	0.0243	0.2274	0.0243	0.2274	0.1613	0.1426	98	160.3333
10.SE	0.0602	0.2258	0.0049	0.3327	0.0003	0.4192	70	2202.4231

The calculation of maximal possible consecutive generations of *Cx. pipiens* s.s./*Cx. torrentium* resulted in a range of 0 to 12 generations per season for the modelling region (Figure 8). Ten to twelve generations were calculated for the southern parts of Portugal, Spain and Italy as on the Mediterranean Islands. Zero to three generations per season were calculated for the most northern parts of Scandinavia and the Alps. The generations in Germany ranged from four to seven. The calculations also depict annual difference in maximum consecutive generations.

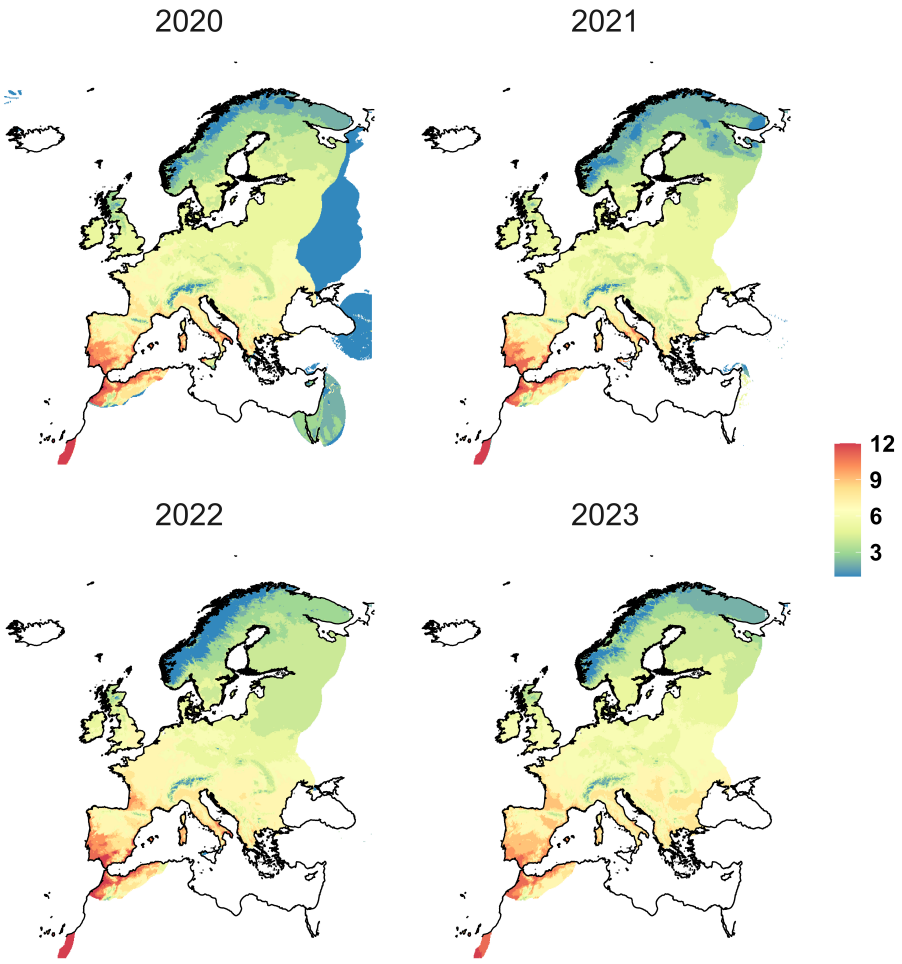

Figure 8: Raster Map of maximum possible number of consecutive generations per season of *Cx. pipiens* s.s./ *Cx. torrentium* over entire Europe

In the sensitivity analysis, we observe that the egg development rate, larva development rate, pupa development rate, host-seeking rate, and the sex ratio at the emergence are positively correlated to the peak of the population of host-seeking adults, indicating a strong contribution to the peak of the population of host-seeking adults (Figure 9 A. However, the egg development rate has the highest contribution to the peak, indicating a high level of uncertainty when its values are changed. On the other hand, the adult mortality rate is highly negatively correlated to the peak of host-seeking adults. Similarly, the mortality rates of mosquitoes in the aquatic stages, larva carrying capacity, and the resting rate of host-seeking females are also negatively correlated to the peak of host-seeking females.

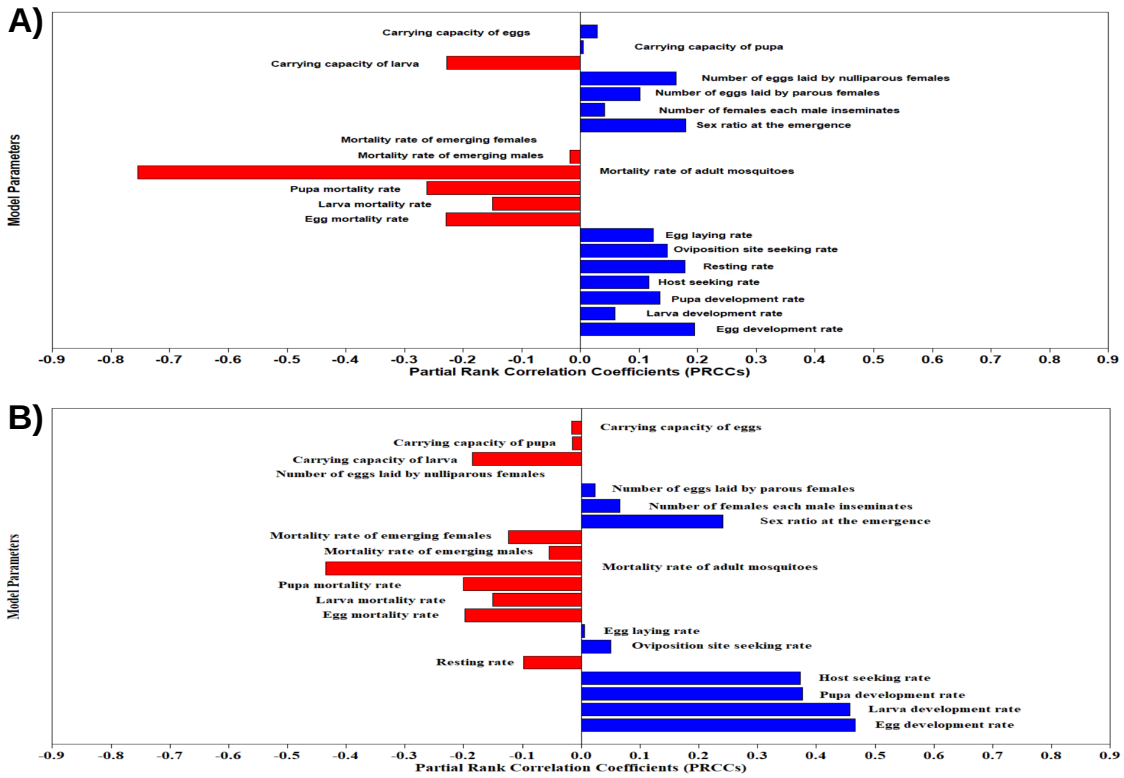

Figure 9: Sensitivity analysis for A) the peak of host-seeking mosquitoes and B) the dynamics of host-seeking mosquitoes.

Moreover, we observe that the egg development rate, sex ratio at emergence, resting rate, and the number of eggs laid by nulliparous females are positively correlated to the overall dynamics of host-seeking adults throughout the simulation period 9 B. On the other hand, the mortality of adult mosquitoes strongly impacts the decline of the population density of host-seeking adults, followed by the mortality rates of mosquitoes in the aquatic stages. The sensitivity analysis results for the peak and overall dynamic are quite similar, but there are slight differences. The negative effect of the adult mortality rate is twice as strong for the overall dynamic than for the abundance peak. While the resting rate is negatively correlated to the abundance peak, it has a slight but positive effect on the overall dynamics. Additionally, the strong positive impact of the host-seeking rate and larvae development rate on the abundance peak is only small for the overall dynamic.

Table 2: Summary statistics for the Pearson correlation analysis for absolute abundances and the temperature aggregated for all sampling sites within the three agro-climatic zones present in Germany

Year	Agro-climate	P-Value	Estimate	Datapoints	Sampling sites
2021	Maritime North	0.0000	0.7652	940	22
2022	Maritime North	0.0000	0.6735	277	11
2023	Pannonial	0.0005	0.6223	178	5
2021	Pannonial	0.0013	0.5859	288	5
2023	Maritime North	0.0059	0.4832	603	12
2016	Pannonial	0.0088	0.6916	36	3
2017	Maritime North	0.0124	0.5022	409	35
2017	Continental	0.0182	0.6410	24	2
2022	Continental	0.0283	0.5841	14	1
2016	Maritime North	0.0412	0.3954	441	37
2016	Continental	0.0476	0.5809	24	2
2022	Pannonial	0.0504	0.3666	143	8
2021	Continental	0.1576	0.4827	29	2
2023	Continental	0.9872	-0.0047	30	1

Discussion

Starting with the model published by Ezanno et al. (2015) we were able reproduce the results from southern France relatively well. Yet the model was not able to produce seasonal dynamics for more temperate regions. This led to us taking a closer look at the temperature dependent mortality and transition rates. While the

linear egg-to-larvae transition rate resulted in suitable values for the Mediterranean, it made the survival off eggs impossible for the temperature range of Germany (Figure 2 A). This was resolved by using a sigmoid function delivering sensical transition rates over a large temperature range. The former larvae mortality rate was a decaying exponential function resulting in the minimal mortality rate over almost the entire temperature range (Figure 2 B). This function was replaced with a piecewise logistic function resulting in the lowest mortality being around 20°C and increasing in both directions gradually. The model shows fell-fitting seasonal dynamics over entire Europe and all life stages. The overwintering life stages, in the model, are gravid females and males. While studies find *Cx. pipiens* s.s./*Cx. torrentium* overwintering in cellars and sheds the proportion of males is extremely low (Sauer et al., 2022). Previously inseminated females overwinter in burrows barns and cellars and are the ones that start the new population by laying eggs in the beginning of the favourable season. The model can pinpoint the seasonal peak of abundance of *Cx. pipiens* s.s./*Cx. torrentium*. The capability of such models to do so was previously shown (Ezanno et al., 2015). In contrast to these publications, our model can do so using daily predictions while they were using monthly averages and therefore only pinpointing the month of peak abundance. Pinpointing the peak of abundance is an important feature of such a model. It can therefore be used to inform pest control management about the best time point for pesticide application. Regarding the start and endpoint of the season, our model shows a similar pattern compared to literature (Marini et al., 2016). In this former publication, the onset of the season depicted by the model was found to be a few weeks prior to the pattern found in field data, while the offset of the season depicted by the model was within one to two weeks before the offset depicted by field data. Although the overall start and endpoints of the season, in our model, deviated significantly from zero, an exact pinpointing was quite common. This is especially true for the endpoint of the season, where the median offset was 0. Especially the start point of the season can be of great importance for vector control measures, since larvicide treatments during the beginning of the favourable season can have lasting impact on the mosquito population (Runge et al., 2021). But since the model is constantly rushing the start point of the season, it could still be used for this purpose although it cannot exactly pinpoint the day.

Although not all sampling sites showed a significant Pearson correlation the overall linear model showed a significant relationship between the number of predicted actually captured mosquito specimens, i.e. capable of

informing about the general phenology of *Cx. pipiens* s.s./*Cx. torrentium*. The model is highly temperature dependent, but it explains 44% more of the variation in the dataset compared to temperature-only model. We see a relationship between the number of data points available for a sample site and the significance of the Pearson correlation. Which raises the question of how many traps per site or how high the temporal resolution has to be, to be able to observe a representative population dynamic? Preceding publications averaged over 15 to 50 traps sampled on a weekly or biweekly basis, reaching Pearson correlations of field data to model output of 0.73 - 0.93 (Tran et al., 2013). In the publication of Ezanno et al. (2015) it was shown that the sampling year where only one trap was used per sampling site had a slightly lower correlation coefficients (mean=0.73, range=0.60-0.81) then the sampling year when they averaged eight traps per sampling site (mean=0.78, range=0.54-0.92) (Ezanno et al., 2015). In our study, most sampling sites were sampled on a weekly basis, with the exception of some sites that were almost sampled daily. From these sampling sites all but one showed a significant positive Pearson correlation (Table 1). The peak in abundance seems to be generally short. Therefore, it can be easily missed by timing, bad weather or Trap user error. The agro-climatic areas can be very useful information not only for crops but also for mosquitoes. They give more information about the lengths of the favourable season and cumulative heat. The modelled population dynamics for these regions were highly correlated with the field data. The two zones without significant correlation were the continental region for the Years 2021 and 2022 (Table 2).For three other years the aggregated data was significantly correlated (2016, 2017 and 2022). The continental region was also the sampling site with the least available data points. Most sampling sites were situated in the Maritime North. This region also had the most sampling sites with high temporal resolution (almost daily). A well-functioning model can be a very useful tool. Informing pest control management and assessing virus transmission risk are two prime examples. Such a model provides valuable ecological insights, including the maximum number of consecutive generations per season (Figure 8). This metric can be used to inform the species habitat range and highlight regions with similar suitability. Furthermore, it can be crucial for assessing the impact of vertical transmission, i.e. the transmission of arboviruses from egg-laying female mosquitoes to their offspring as is known to occur for WNV in *Cx pipiens* s.s./*Cx. torrentium* mosquitoes (Nelms et al., 2013). While the impact of vertical transmission on the overall WNV transmission cycle is

not entirely understood, it could play a major role as virus reservoir host over the winter months.

Conclusion

The *Cx. pipiens* s.s./*Cx. torrentium* process-based model serves as a useful tool for predicting the abundance of host-seeking female mosquitoes. The model effectively identifies peak abundance, making it highly valuable for vector control purposes. Moreover, it operates across a comprehensive environmental data set spanning the entire European continent, highlighting its applicability on a large scale.

Acknowledgements

We gratefully acknowledge the voluntary helpers who supported the field work, and Lisa J. Winter for her help during laboratory work.

Funding

This project is funded through the Federal Ministry of Education and Research of Germany, with grant number 01Kl2022.

Supplements

Table 3: Summary statistics for the correlation analysis for absolute abundances, relative abundances and the temperature for all sampling sites

ID	P-value model	Estimate model	P-value temperature	Estimate temperature	Capture days	Captured mosquitoes
1.PG	0.0000	0.4511	0.0000	0.4616	112	1927.1817
10.PG	0.0000	0.3947	0.0029	0.2483	142	627.3571
3.PR	0.0000	0.4965	0.0000	0.5066	61	153.4952
45.PR	0.0000	0.5302	0.0012	0.3611	78	425.0476
8.PG	0.0000	0.2949	0.0000	0.3186	544	4158.0000
9.PG	0.0000	0.5468	0.0000	0.5744	74	688.9167
9.PR	0.0000	0.5838	0.0000	0.5939	46	108.7500
3.PG	0.0001	0.3811	0.0001	0.3765	104	1179.9500
47.PG	0.0004	0.7027	0.0029	0.6163	21	340.0000
G15S86	0.0007	0.8358	0.0959	0.5025	12	503.0000
45.SC	0.0008	0.4283	0.0082	0.3440	58	2007.0000
G15S33	0.0012	0.8150	0.5173	0.2076	12	61.0000
14.PG	0.0017	0.5049	0.0260	0.3708	36	226.0000
7.PR	0.0019	0.7128	0.0155	0.5930	16	230.0000
1.PR	0.0028	0.2976	0.1393	0.1497	99	569.8929
8.PR	0.0038	0.2913	0.0006	0.3415	97	855.7619
G15S21	0.0048	0.8064	0.1260	0.5170	10	63.0000
G15S28	0.0066	0.7333	0.0474	0.5814	12	78.0000
25.PG	0.0070	0.4416	0.0132	0.4090	36	75.0000
48.PG	0.0076	0.4376	0.0010	0.5257	36	289.0000
43.SE	0.0108	0.5845	0.2753	0.2718	18	47.0000

ID	P-value model	Estimate model	P-value temperature	Estimate temperature	Capture days	Captured mosquitoes
G10S51	0.0128	0.6914	0.0032	0.7728	12	67.0000
11.PG	0.0133	0.2332	0.0666	0.1740	112	391.0000
13.PG	0.0162	0.6497	0.0231	0.6225	13	89.0000
G11S29	0.0177	0.6673	0.4143	0.2600	12	933.0000
G11S47	0.0188	0.6628	0.1534	0.4390	12	684.0000
G15S87	0.0191	0.6615	0.2284	0.3760	12	31.0000
18.PG	0.0196	0.3169	0.0066	0.3656	54	281.0000
19.PG	0.0205	0.3848	0.1959	0.2207	36	120.0000
G10S34	0.0205	0.6560	0.1184	0.4752	12	38.0000
G10S42	0.0233	0.6458	0.5649	0.1850	12	48.0000
30.PG	0.0243	0.2274	0.1613	0.1426	98	160.3333
G11S35	0.0278	0.6309	0.4413	0.2458	12	522.0000
35.SE	0.0283	0.5841	0.1185	0.4366	14	95.0000
G10S36	0.0286	0.6285	0.2868	0.3352	12	1263.0000
G15S24	0.0298	0.6248	0.9461	0.0219	12	338.0000
G11S59	0.0332	0.6154	0.1830	0.4122	12	256.0000
G15S22	0.0336	0.6143	0.5961	0.1706	12	421.0000
G15S98	0.0387	0.6011	0.1183	0.4754	12	32.0000
G10S60	0.0408	0.5961	0.7500	0.1030	12	229.0000
G11S49	0.0408	0.5960	0.1654	0.4278	12	1313.0000
G11S27	0.0463	0.5838	0.7771	0.0916	12	175.0000
G11S26	0.0467	0.5829	0.6755	0.1351	12	422.0000
G15S85	0.0478	0.5805	0.5294	0.2018	12	1612.0000
G10S38	0.0485	0.5791	0.1146	0.4796	12	548.0000
G11S34	0.0552	0.5657	0.3299	0.3081	12	1308.0000

ID	P-value model	Estimate model	P-value temperature	Estimate temperature	Capture days	Captured mosquitoes
10.SE	0.0602	0.2258	0.0003	0.4192	70	2202.4231
G11S45	0.0612	0.5548	0.6873	0.1299	12	373.0000
G11S18	0.0629	0.5518	0.3336	0.3059	12	277.0000
G10S41	0.0646	0.5488	0.0344	0.6122	12	41.0000
G15S41	0.0656	0.5471	0.0397	0.5986	12	380.0000
G10S25	0.0694	0.5409	0.0928	0.5066	12	378.0000
49.PG	0.0725	0.4766	0.0030	0.7096	15	108.0000
G10S29	0.0727	0.5356	0.6721	0.1366	12	40.0000
G11S32	0.0780	0.5274	0.3844	0.2764	12	229.0000
15.SE	0.0809	0.2492	0.0816	0.2487	50	502.0000
2.PR	0.0813	0.5008	0.0415	0.5712	13	119.5238
G15S20	0.0847	0.5177	0.1590	0.4336	12	1503.0000
G11S56	0.0894	0.5112	0.6539	0.1446	12	374.0000
39.SE	0.0920	0.5321	0.9468	0.0229	11	591.0000
G11S50	0.0953	0.5033	0.2697	0.3466	12	604.0000
G15S42	0.0960	0.5025	0.7096	0.1203	12	121.0000
G15S27	0.0999	0.4974	0.3892	0.2738	12	57.0000
G11S62	0.1012	0.4958	0.3723	0.2833	12	218.0000
G11S54	0.1040	0.4923	0.3145	0.3176	12	701.0000
G11S24	0.1083	0.4870	0.0121	0.6953	12	85.0000
G10S28	0.1100	0.4850	0.4216	0.2561	12	266.0000
G11S25	0.1241	0.4689	0.5256	0.2036	12	949.0000
4.PR	0.1362	0.2835	0.0677	0.3439	29	802.3718
G11S31	0.1402	0.4520	0.3194	0.3145	12	1511.0000
G15S82	0.1402	0.4520	0.2981	0.3279	12	153.0000

ID	P-value model	Estimate model	P-value temperature	Estimate temperature	Capture days	Captured mosquitoes
16.SE	0.1432	0.3830	0.2449	0.3086	16	764.0000
G15S97	0.1556	0.4368	0.8895	0.0450	12	36.0000
G11S19	0.1557	0.4368	0.3162	0.3165	12	4491.0000
G15S30	0.1576	0.4350	0.9652	-0.0141	12	1843.0000
G11S17	0.1632	0.4298	0.3785	0.2797	12	1542.0000
G11S57	0.1654	0.4278	0.6531	0.1449	12	932.0000
G11S44	0.1671	0.4262	0.3804	0.2787	12	603.0000
31.PG	0.1692	0.1552	0.0001	0.4271	80	280.2524
G11S23	0.1747	0.4194	0.4129	0.2608	12	3780.0000
G15S99	0.1751	0.4191	0.0383	0.6020	12	61.0000
G11S55	0.1774	0.4170	0.1243	0.4688	12	389.0000
G11S20	0.1850	0.4105	0.3349	0.3051	12	200.0000
20.PG	0.1884	0.2720	0.1239	0.3159	25	127.0000
G10S62	0.1926	0.4042	0.5259	0.2035	12	121.0000
G15S40	0.1953	0.4019	0.8521	-0.0604	12	729.0000
4.PG	0.2038	0.2525	0.1534	0.2825	27	363.6071
G11S53	0.2072	0.3923	0.4449	0.2439	12	2953.0000
G11S21	0.2077	0.3919	0.5494	0.1923	12	353.0000
G15S34	0.2146	0.3865	0.1322	0.4602	12	33.0000
7.PG	0.2165	0.2284	0.2905	0.1960	31	342.0000
G11S46	0.2270	0.3770	0.2895	0.3334	12	890.0000
11.PR	0.2358	0.2777	0.1660	0.3222	20	463.0000
G10S53	0.2395	0.3678	0.0693	0.5411	12	33.0000
G11S52	0.2506	0.3599	0.6526	0.1452	12	972.0000
G15S83	0.2541	0.3574	0.6921	0.1279	12	922.0000

ID	P-value model	Estimate model	P-value temperature	Estimate temperature	Capture days	Captured mosquitoes
16.PG	0.2878	0.1188	0.4730	-0.0803	82	254.0000
G15S29	0.2978	0.3281	0.4390	0.2470	12	6539.0000
G11S48	0.3048	0.3237	0.3157	0.3168	12	1933.0000
G15S23	0.3069	0.3223	0.6096	0.1644	12	566.0000
G11S22	0.3081	-0.3216	0.4108	0.2620	12	1080.0000
G11S28	0.3095	0.3207	0.5062	0.2130	12	1653.0000
G15S31	0.3167	0.3162	0.9239	0.0310	12	334.0000
23.PG	0.3180	0.2577	0.0163	0.5728	17	859.0000
2.PG	0.3462	0.2436	0.6640	0.1137	17	153.7239
G11S33	0.3508	0.2957	0.5314	0.2008	12	35.0000
G11S64	0.3584	0.2912	0.6781	0.1340	12	52.0000
G11S63	0.3644	0.2878	0.5967	0.1703	12	93.0000
G11S30	0.3879	0.2745	0.9972	-0.0012	12	1237.0000
G15S91	0.4440	0.2444	0.7951	0.0841	12	430.0000
G11S60	0.4565	0.2379	0.7971	-0.0832	12	85.0000
34.PG	0.4707	0.2434	0.1656	-0.4494	11	36.5000
G15S92	0.4854	0.2233	0.0293	0.6263	12	127.0000
G11S51	0.4988	0.2167	0.1192	0.4744	12	123.0000
21.PG	0.5506	0.1557	0.9672	-0.0108	17	40.0000
5.PR	0.5973	-0.1795	0.2042	-0.4151	11	108.6429
24.PG	0.6675	-0.0866	0.7327	0.0689	27	222.0000
15.PG	0.7049	0.1475	0.8302	0.0839	9	65.0000
33.SE	0.7598	-0.1045	0.9700	-0.0129	11	56.0000
G11S58	0.7651	0.0966	0.2142	0.3868	12	89.0000
17.SE	0.7865	-0.1149	0.2605	-0.4523	8	78.0000

ID	P-value model	Estimate model	P-value temperature	Estimate temperature	Capture days	Captured mosquitoes
G11S61	0.8302	-0.0694	0.5793	-0.1783	12	66.0000
G15S94	0.9842	0.0064	0.0122	0.6944	12	158.0000

Table 4: Definition an sources of parameters used in the process-based model

Variable	Definition	Value	Location
$\phi_1(T)$	egg hatching rate	$\frac{0.5}{1+e^{0.1(10-T)}}$	calculated
$\phi_2(T)$	larva development rate	$\frac{0.5}{1+e^{0.1(10-T)}}$	calculated
$\phi_3(T)$	pupa development rate	$\frac{0.5}{1+e^{0.1(10-T)}}$	calculated
ϕ_4	host seeking rate	0.4	(Tran et al., 2013)
ϕ_5	resting rate	0.2	(Tran et al., 2013)
$\phi_6(T)$	oviposition site seeking rate	$\min\left(\frac{T-T_6}{TDDAg}, 0\right)$	(Ezanno et al., 2015; Tran et al., 2013)
ϕ_7	egg laying rate	2	(Tran et al., 2013)
μ_E	Egg mortality rate	0.0262	(Ezanno et al., 2015)
$\mu_L(T)$	Larva mortality rate	$\frac{0.86}{1+e^{-0.2(45-T)}}$	calculated
$\mu_P(T)$	Pupa mortality rate	$\frac{0.86}{1+e^{-0.2(45-T)}}$	calculated
$\mu_A(T)$	Natural mortality rate of adult mosquito	$\max(\mu_A, -0.005941+0.002965T)$	(Tran et al., 2013)
α	sex ratio at the emergence stage	0.5	(Altizer et al., 2013; Ezanno et al., 2015)
T_6	Minimal temperature needed for egg maturation (^0C)	9.8	(Ahumada et al., 2004; Balenghien et al., 2008; Ezanno et al., 2015)
T_{DDAg}	Number of degree-days needed for egg maturation (^0C)	64.4	(Ahumada et al., 2004; Balenghien et al., 2008; Ezanno et al., 2015)

References

Roumen Anguelov, Claire Dufourd, and Yves Dumont. Mathematical model for pest–insect control using mating disruption and trapping. *Applied Mathematical Modelling*, 52:437–457, 2017. doi: 10.1016/j.apm.2017.07.060.

Monica Asman. Observations of mating behavior in *Culex tarsalis*. *Annals of the Entomological Society of America*, 68(5):777–778, 1975. doi: 10.1093/aesa/68.5.777.

Norbert Becker, Hanna Jöst, Ute Ziegler, Martin Eiden, Dirk Höper, Petra Emmerich, Elisabeth Fichet-Calvet, Deborah U Ehichioya, Christina Czajka, Martin Gabriel, et al. Epizootic emergence of Usutu virus in wild and captive birds in Germany. *PloS One*, 7(2):e32604, 2012.

Norbert Becker, Dušan Petrić, Marija Zgomba, Clive Boase, Minoo B Madon, Christine Dahl, and Achim Kaiser. *Mosquitoes: identification, ecology and control*. Springer Nature, 2020.

Sally M Blower and Hadi Dowlatabadi. Sensitivity and uncertainty analysis of complex models of disease transmission: an hiv model, as an example. *International Statistical Review/Revue Internationale de Statistique*, pages 229–243, 1994.

Kostas Bourtzis, Stephen L Dobson, Zhiyong Xi, Jason L Rasgon, Maurizio Calvitti, Luciano A Moreira,

Hervé C Bossin, Riccardo Moretti, Luke Anthony Baton, Grant L Hughes, et al. Harnessing mosquito–*Wolbachia* symbiosis for vector and disease control. *Acta Tropica*, 132:S150–S163, 2014.

Oliver J Brady, Peter W Gething, Samir Bhatt, Jane P Messina, John S Brownstein, Anne G Hoen, Catherine L Moyes, Andrew W Farlow, Thomas W Scott, and Simon I Hay. Refining the global spatial limits of dengue virus transmission by evidence-based consensus. 2012.

Daniel Cadar, Renke Lühken, Henk van der Jeugd, Mutien Garigliany, Ute Ziegler, Markus Keller, Jennifer Lahoreau, Lars Lachmann, Norbert Becker, Marja Kik, et al. Widespread activity of multiple lineages of Usutu virus, western Europe, 2016. *Eurosurveillance*, 22(4):30452, 2017.

Priscilla Cailly, Annelise Tran, Thomas Balenghien, Grégory L'Ambert, Céline Toty, and Pauline Ezanno. A climate-driven abundance model to assess mosquito control strategies. *Ecological Modelling*, 227:7–17, 2012. ISSN 0304-3800. doi: 10.1016/j.ecolmodel.2011.10.027.

Andrej Ceglar, Matteo Zampieri, Andrea Toreti, and Franciscus Dentener. Observed northward migration of agro-climate zones in Europe will further accelerate under climate change. *Earth's Future*, 7(9):1088–1101, 2019.

Richard C Cornes, Gerard van der Schrier, Else JM van den Besselaar, and Philip D Jones. An ensemble version of the E-OBS temperature and precipitation data sets. *Journal of Geophysical Research: Atmospheres*, 123(17):9391–9409, 2018.

Tatiana Sergeevna Detinova, Douglas S Bertram, World Health Organization, et al. *Age-grouping methods in Diptera of medical importance, with special reference to some vectors of malaria*. World Health Organization, 1962.

P. Ezanno, M. Aubry-Kientz, S. Arnoux, P. Cailly, G. L'Ambert, C. Toty, T. Balenghien, and A. Tran. A generic weather-driven model to predict mosquito population dynamics applied to species of *Anopheles*, *Culex* and *Aedes* genera of southern France. *Preventive Veterinary Medicine*, 120(1):39–50, 2015. doi: 10.1016/j.prevetmed.2014.12.018.

Garrett Grolemund and Hadley Wickham. Dates and times made easy with lubridate. *Journal of Statistical Software*, 40(3):1–25, 2011. URL https://www.jstatsoft.org/v40/i03/.

Alexander Hoare, David G Regan, and David P Wilson. Sampling and sensitivity analyses tools (SaSAT) for computational modelling. *Theoretical Biology and Medical Modelling*, 5:1–18, 2008.

Stephanie Jansen, Anna Heitmann, Renke Lühken, Mayke Leggewie, Michelle Helms, Marlis Badusche, Giada Rossini, Jonas Schmidt-Chanasit, and Egbert Tannich. *Culex torrentium*: A potent vector for the transmission of West Nile virus in central Europe. *Viruses*, 11(6):492, 2019.

Alboukadel Kassambara. *rstatix: Pipe-Friendly Framework for Basic Statistical Tests*, 2023. URL https://CRAN.R-project.org/package=rstatix. R package version 0.7.2.

Mathieu Legros, Alun L. Lloyd, Yunxin Huang, and Fred Gould. Density-dependent intraspecific competition in the larval stage of *Aedes aegypti* (diptera: *Culicidae*): Revisiting the current paradigm. *Journal of Medical Entomology*, 46(3):409–419, 2009. doi: 10.1603/033.046.0301.

Angelina Mageni Lutambi, Melissa A. Penny, Thomas Smith, and Nakul Chitnis. Mathematical modelling of mosquito dispersal in a heterogeneous environment. *Mathematical Biosciences*, 241(2):198–216, 2013. doi: 10.1016/j.mbs.2012.11.013.

Giovanni Marini, Piero Poletti, Mario Giacobini, Andrea Pugliese, Stefano Merler, and Roberto Rosà. The role of climatic and density dependent factors in shaping mosquito population dynamics: the case of *Culex pipiens* in northwestern Italy. *PLoS One*, 11(4):e0154018, 2016.

Brittany M Nelms, Ethan Fechter-Leggett, Brian D Carroll, Paula Macedo, Susanne Kluh, and William K Reisen. Experimental and natural vertical transmission of West Nile virus by California *Culex* (diptera: *Culicidae*) mosquitoes. *Journal of medical entomology*, 50(2):371–378, 2013.

R Core Team. *R: A Language and Environment for Statistical Computing*. R Foundation for Statistical Computing, Vienna, Austria, 2016. URL https://www.R-project.org/.

Manuela Runge, Salum Mapua, Ismail Nambunga, Thomas A Smith, Nakul Chitnis, Fredros Okumu, and

Emilie Pothin. Evaluation of different deployment strategies for larviciding to control malaria: a simulation study. *Malaria journal*, 20:1–14, 2021.

FG Sauer, E Timmermann, U Lange, R Lühken, and E Kiel. Effects of hibernation site, temperature, and humidity on the abundance and survival of overwintering *Culex pipiens pipiens* and *Anopheles messeae* (diptera: *Culicidae*). *Journal of Medical Entomology*, 59(6):2013–2021, 2022.

Annelise Tran, Grégory L'ambert, Guillaume Lacour, Romain Benoît, Marie Demarchi, Myriam Cros, Priscilla Cailly, Mélaine Aubry-Kientz, Thomas Balenghien, and Pauline Ezanno. A rainfall-and temperature-driven abundance model for *Aedes albopictus* populations. *International journal of Environmental Research and Public Health*, 10(5):1698–1719, 2013.

Magdalena Laura Wehmeyer, Linda Jaworski, Hanna Jöst, Tatiana Șulețco, Leif Rauhöft, Sara M Martins Afonso, Markus Neumann, Konstantin Kliemke, Unchana Lange, Ellen Kiel, et al. Host attraction and host feeding patterns indicate generalist feeding of *Culex pipiens* s.s. and *Cx. torrentium*. *Parasites & Vectors*, 17(1):369, 2024.

WHO et al. World malaria report 2022. geneva: World health organization; 2022. licence: Cc by-nc-sa 3.0 igo. Technical report, accessed 3–1–2023). https://www. who. int/teams/global-malaria-programme …, 2022.

Hadley Wickham. *ggplot2: Elegant Graphics for Data Analysis*. Springer-Verlag New York, 2016. ISBN 978-3-319-24277-4. URL https://ggplot2.tidyverse.org.

Hadley Wickham. *stringr: Simple, Consistent Wrappers for Common String Operations*, 2023. URL https://CRAN.R-project.org/package=stringr. R package version 1.5.1.

Hadley Wickham, Romain François, Lionel Henry, Kirill Müller, and Davis Vaughan. *dplyr: A Grammar of Data Manipulation*, 2023a. URL https://CRAN.R-project.org/package=dplyr. R package version 1.1.4.

Hadley Wickham, Thomas Lin Pedersen, and Dana Seidel. *scales: Scale Functions for Visualization*, 2023b. URL https://CRAN.R-project.org/package=scales. R package version 1.3.0.

Hadley Wickham, Davis Vaughan, and Maximilian Girlich. *tidyr: Tidy Messy Data*, 2024. URL https://CRAN.R-project.org/package=tidyr. R package version 1.3.1.

Yihui Xie. knitr: A general-purpose tool for dynamic report generation in r. *R package version*, 1(1), 2013.

Ute Ziegler, Renke Lühken, Markus Keller, Daniel Cadar, Elisabeth van der Grinten, Friederike Michel, Kerstin Albrecht, Martin Eiden, Monika Rinder, Lars Lachmann, et al. West Nile virus epizootic in Germany, 2018. *Antiviral research*, 162:39–43, 2019.

Ute Ziegler, Pauline Dianne Santos, Martin H Groschup, Carolin Hattendorf, Martin Eiden, Dirk Höper, Philip Eisermann, Markus Keller, Friederike Michel, Robert Klopfleisch, et al. West Nile virus epidemic in Germany triggered by epizootic emergence, 2019. *Viruses*, 12(4):448, 2020.